

## **Electronic modulation of Co<sub>2</sub>P nanoneedle arrays by doping of transition metal Cr atom for urea oxidation reaction**

Xinyu Li<sup>a</sup>, Xiaoqiang Du<sup>a\*</sup> and Xiaoshuang Zhang<sup>b</sup>

<sup>a</sup> School of Chemical Engineering and Technology, Shanxi Key Laboratory of High Performance Battery Materials and Devices, North University of China, Xueyuan road 3, Taiyuan 030051, People's Republic of China. E-mail: duxq16@nuc.edu.cn

<sup>b</sup> School of Science, North University of China, Xueyuan road 3, Taiyuan 030051, People's Republic of China.

### **Materials and chemicals**

Concentrated hydrochloric acid (HCl, 12 mol/L), acetone (CO(CH<sub>3</sub>)<sub>2</sub>, >99%), Cobalt nitrate hexahydrate (Co(NO<sub>3</sub>)<sub>2</sub>·6H<sub>2</sub>O, >99%), Chromium nitrate hexahydrate (Cr(NO<sub>3</sub>)<sub>3</sub>·9H<sub>2</sub>O, >99%), Ammonium fluoride (NH<sub>4</sub>F, >99%), urea (CO(NH<sub>2</sub>)<sub>2</sub>, >99%) and potassium hydroxide (KOH, >99%) were purchased from Sinopharm Chemical Reagent Ltd and could be used directly without further purification. Nickel foam (NF, 1.0 mm in thickness) was served as substrates of target catalysts with pretreatment before use. Furthermore, sufficient ultrapure water was prepared throughout the experiments.

### **DFT calculation**

The DFT calculations were performed using the Cambridge Sequential Total Energy Package (CASTEP) with the plane-wave pseudo-potential method. The geometrical structures of the (110) plane of Cr<sub>0.3</sub>-Co<sub>2</sub>P, Cr<sub>0.4</sub>-Co<sub>2</sub>P and Cr<sub>0.5</sub>-Co<sub>2</sub>P were optimized by the generalized gradient approximation (GGA) methods. The Revised Perdew-Burke-Ernzerh of (RPBE) functional was used to treat the electron exchange correlation interactions. A Monkhorst Pack grid k-points of 5\*3\*1 of Cr<sub>0.3</sub>-Co<sub>2</sub>P, Cr<sub>0.4</sub>-Co<sub>2</sub>P and Cr<sub>0.5</sub>-Co<sub>2</sub>P, a plane-wave basis set cut-off energy of 500 eV were used for integration of the Brillouin zone. The structures were optimized for energy and force convergence set at 0.05 eV/Å and 2.0×10<sup>-5</sup> eV, respectively. The vacuum space was up to 0.002 Å to eliminate periodic interactions.

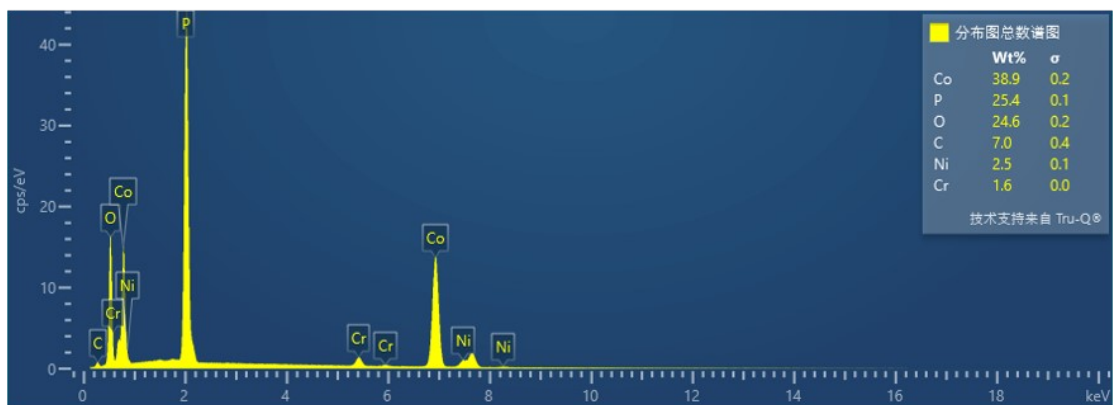


Fig. S1 EDS spectra of the  $\text{Cr}_{0.4}\text{-Co}_2\text{P/NF}$  material.

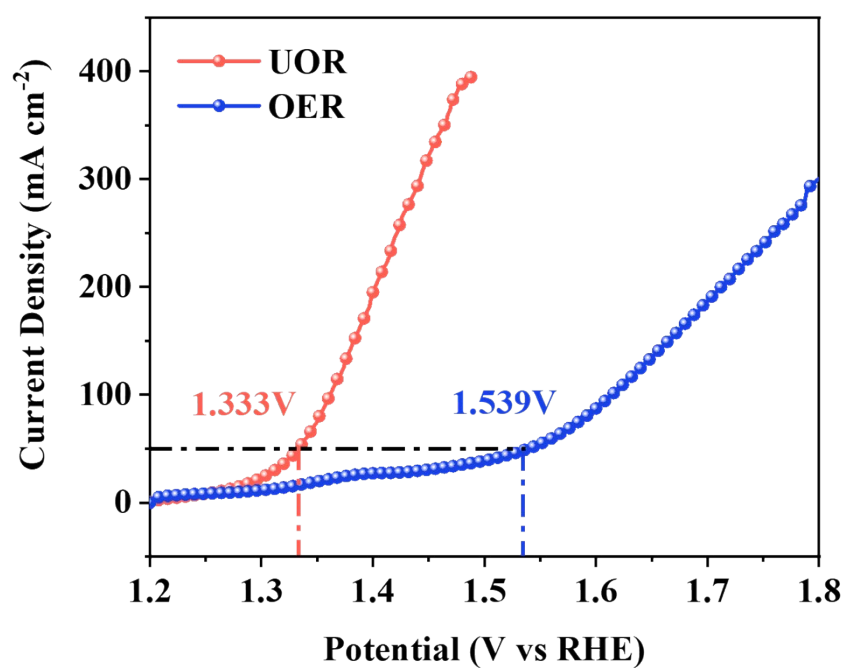
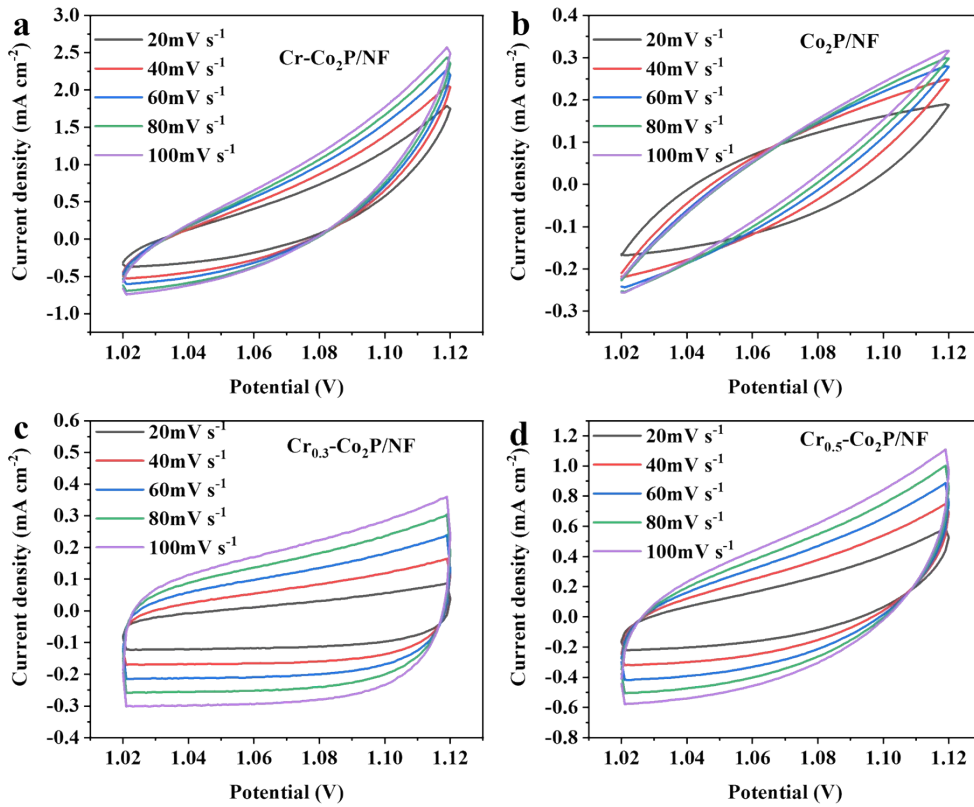
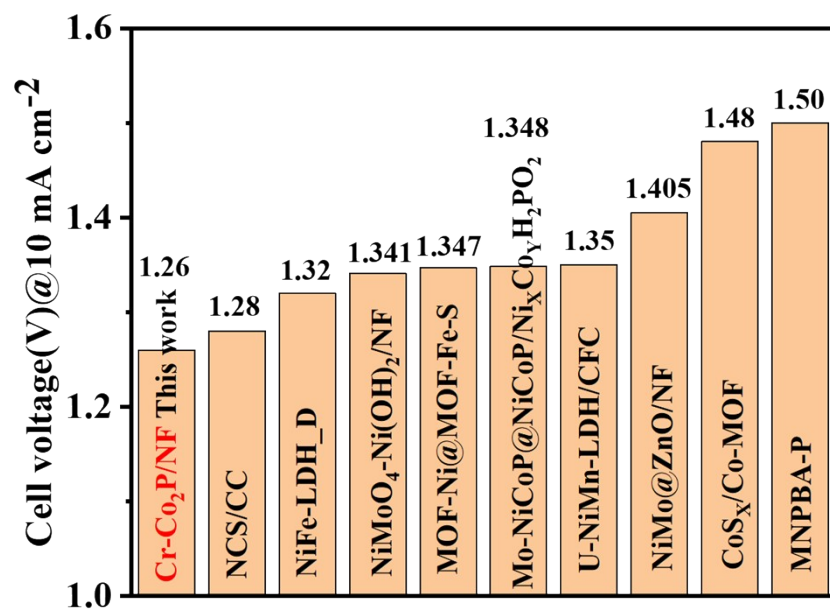


Fig. S2 Comparison of overpotentials of UOR and OER.



**Fig. S3** In 1.0 M KOH + 0.5 M urea, UOR cyclic voltammograms of a)  $\text{Cr}_{0.4}\text{-Co}_2\text{P/NF}$ , b)  $\text{Co}_2\text{P/NF}$ , c)  $\text{Cr}_{0.3}\text{-Co}_2\text{P/NF}$  and d)  $\text{Cr}_{0.5}\text{-Co}_2\text{P/NF}$  at the different scan rates varying from 20 to 100  $\text{mV}\cdot\text{s}^{-1}$ .



**Fig. S4** Comparison of urea electrolysis performance with previously reported electrocatalysts [1-9]

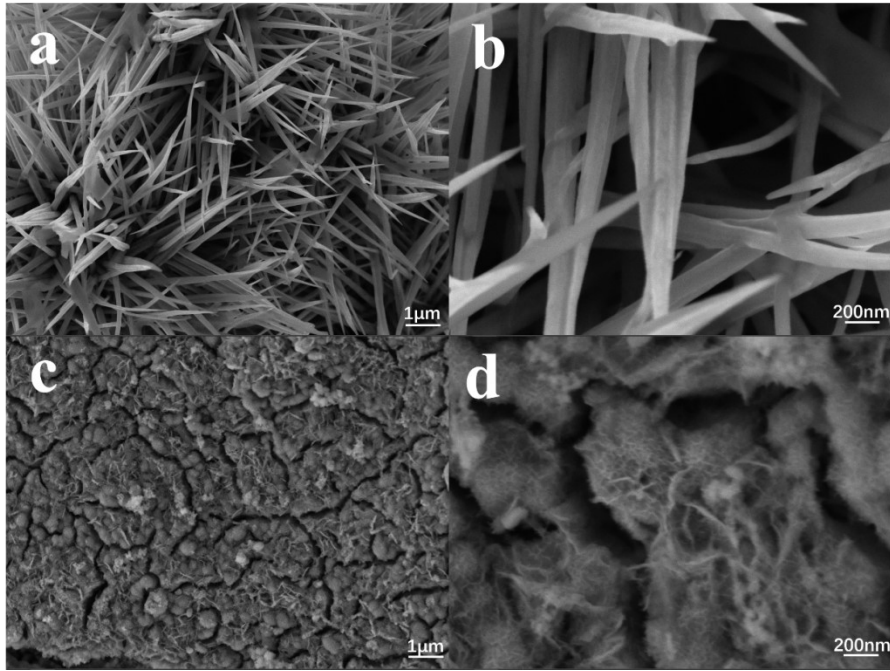


**Fig. S5** SEM of  $\text{Cr}_{0.4}\text{-Co}_2\text{P/NF}$  before (a-b) and after (c-d) 12 h for UOR.

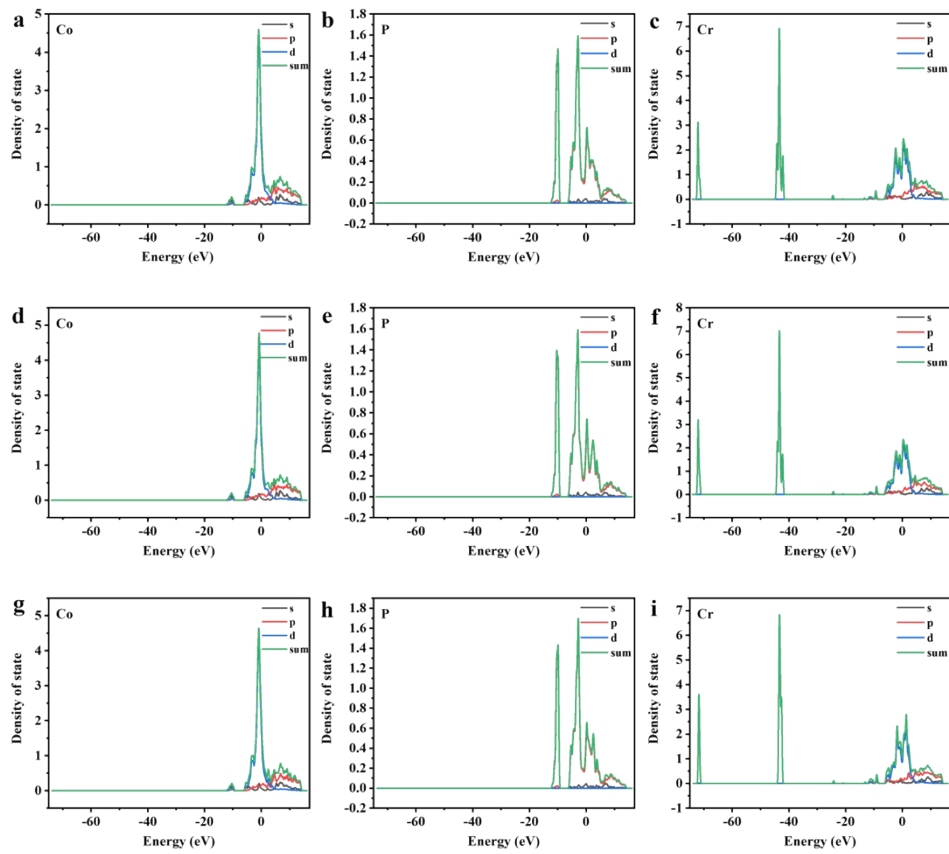


**Fig. S6** The partial density of states for the  $\text{Cr}_{0.3}\text{-Co}_2\text{P}$ , (a) Co, (b) P and (c) Cr; the  $\text{Cr}_{0.4}\text{-Co}_2\text{P}$ , (d) Co, (e) P and (f) Cr; the  $\text{Cr}_{0.5}\text{-Co}_2\text{P}$ , (g) Co, (h) P and (i) Cr.

**Table S1** the molar amount of every atom for the Cr<sub>0.4</sub>-Co<sub>2</sub>P/NF catalyst

Element	Mass fraction %	Atomic fraction %
Co	8.38	5.45
Cr	0.62	0.5
P	19.64	34.87
O	58.07	48.54
C	13.29	10.63

[1] C.Y. Zhang, T.T. Chen, H. Zhang, Z.H. Li, J.C. Hao, Hydrated-Metal-Halide-Based Deep-Eutectic-Solvent-Mediated NiFe Layered Double Hydroxide: An Excellent Electrocatalyst for Urea Electrolysis and Water Splitting, *Chem-Asian. J.*, 14 (2019) 2995-3002.

[2] J. Cao, H.C. Li, R.T. Zhu, L. Ma, K.C. Zhou, Q.P. Wei, F.H. Luo, Improved hydrogen generation via a urea-assisted method over 3D hierarchical NiMo-based composite microrod arrays, *J.Alloy.Comp.*, 844 (2020).

[3] P. Hao, W.Q. Zhu, L.Y. Li, J. Tian, J.F. Xie, F.C. Lei, G.W. Cui, Y.Q. Zhang, B. Tang, Nickel incorporated Co<sub>9</sub>S<sub>8</sub> nanosheet arrays on carbon cloth boosting overall urea electrolysis, *Electrochim. Acta*, 338 (2020).

[4] S.N. Hu, H.M. Wu, C.Q. Feng, Y. Ding, Synthesis of non-noble NiMoO<sub>4</sub>-Ni(OH)<sub>2</sub>/NF bifunctional electrocatalyst and its application in water-urea electrolysis, *Int. J. Hydrogen Energy*, 45 (2020) 21040-21050.

- [5] H.Z. Xu, K. Ye, K. Zhu, Y.Y. Gao, J.L. Yin, J. Yan, G.L. Wang, D.X. Cao, Transforming Carnation-Shaped MOF-Ni to Ni-Fe Prussian Blue Analogue Derived Efficient Bifunctional Electrocatalyst for Urea Electrolysis, *ACS Sustain. Chem. Eng.*, 8 (2020) 16037-16045.
- [6] H.Z. Xu, K. Ye, K. Zhu, J.L. Yin, J. Yan, G.L. Wang, D.X. Cao, Efficient bifunctional catalysts synthesized from three-dimensional Ni/Fe bimetallic organic frameworks for overall urea electrolysis, *Dalton Transactions*, 49 (2020) 5646-5652.
- [7] H.Z. Xu, K. Ye, K. Zhu, J.L. Yin, J. Yan, G.L. Wang, D.X. Cao, Template-directed assembly of urchin-like CoS<sub>x</sub>/Co-MOF as an efficient bifunctional electrocatalyst for overall water and urea electrolysis, *Inorg. Chem. Front.*, 7 (2020) 2602-2610.
- [8] G.Q. Liu, C. Huang, Z.H. Yang, J.H. Su, W.X. Zhang, Ultrathin NiMn-LDH nanosheet structured electrocatalyst for enhanced electrocatalytic urea oxidation, *Applied Catalysis a-General*, 614 (2021).
- [9] C.Y. Zhang, X.Q. Du, X.S. Zhang, Controlled synthesis of three-dimensional branched Mo-NiCoP@NiCoP/NiXCoYH<sub>2</sub>PO<sub>2</sub> core/shell nanorod heterostructures for high-performance water and urea electrolysis, *Int. J. Hydrogen Energy*, 47 (2022) 10825-10836.